



1

1 **CRUX-1.0: An automatic GHG and Ozone observation system for** 2 **inland Antarctica Plateau**

3 **Biao Tian^{1,2}, Minghu Ding^{*1,7}, Kongju Zhu¹, Xu Yao³, Yixi Zhao¹, Wenqian Zhang¹, Diyi**
4 **Yang⁴, Weijun Sun⁵, Yining Yu¹, Shoudong Zhao¹, Yige Cui¹, Chuanjin Li³, Jie Tang¹, Cunde**
5 **Xiao⁶, Tong Zhu², Renhe Zhang⁷**

6 ¹ State Key Laboratory of Disaster Weather Science and Technology, Chinese Academy of
7 Meteorological Sciences, Beijing 100081, China

8 ² College of Environmental Sciences and Engineering, Peking University, Beijing 100871, China

9 ³ Polar Research Institute of China, Shanghai, 200136, China

10 ⁴ Haining Meteorological Bureau, Haining 314400, China

11 ⁵ College of Geography and Environment, Shandong Normal University, Jinan, 250014, China

12 ⁶ State Key Laboratory of Earth Surface Processes and Resource Ecology, Beijing Normal
13 University, Beijing 100875, China

14 ⁷ Key Laboratory of Polar Atmosphere-ocean-ice System for Weather and Climate, Ministry of
15 Education, Shanghai 200438, China

16 *Corresponding authors. E-mail: dingminghu@foxmail.com (Minghu Ding)

17

18 **Abstract:** Antarctic inland regions, as critical hubs for global climate change monitoring, suffer
19 from a lack of reliable long-term greenhouse gas (GHG) observation systems due to extreme low
20 temperatures, strong winds, and limited logistical/energy support. To address this gap, the
21 CRUX-1.0 automatic observation system was developed and deployed at Taishan Station (inland
22 Antarctic Plateau) during the 39th and 40th CHINARE expeditions, targeting simultaneous
23 monitoring of CO₂ and surface ozone (O₃). Integrating four core subsystems—analysis, calibration,
24 temperature control, and data communication—the system is specifically engineered for harsh
25 polar environments with low power consumption (<350 W) and autonomous operation capability.
26 The operational analysis based on A one month continuous field experiment showed its stable
27 performance: CO₂ measurements achieved a coefficient of variation (CV) <6% (nearing 0%
28 post-calibration), while O₃ measurements maintained a CV <5.6%. The average concentrations
29 (CO₂: 420.3±1.5 ppm; O₃: 20.1±0.8 ppb) closely aligned with regional background levels and
30 South Pole Station data, confirming high reliability. With its robust adaptability, CRUX-1.0 could
31 be extended to other polar or high-altitude regions, further enhancing the global atmospheric
32 monitoring network's coverage and capability.

33 **Keywords:** GHG, Ozone, automatic observation system, Antarctica

34

35 **1. Introduction**

36 Observing atmospheric composition and greenhouse gases is a critical global issue, as it serves as
37 a key benchmark for assessing global changes and formulating policies such as the Paris
38 Agreement and Conference of the Parties (COP) negotiations. Currently, global atmospheric
39 background stations provide a significant amount of observational data, but their distribution
40 remains uneven. In fact, there are notable disparities in greenhouse gas concentrations across
41 different regions. For example, high-latitude and polar regions, including Antarctica, suffer from a
42 lack of observation stations, making it difficult to monitor the atmospheric composition in these



2

43 areas (Das et al., 2016; Liu et al., 2024). The absence of sufficient observation capacity in these
44 regions highlights the need for enhanced monitoring systems. In particular, the challenging
45 environmental conditions and logistical difficulties in these regions necessitate advancements in
46 observation technologies and improved support for maintaining such systems. Given these
47 challenges, there is a growing demand for increasing the capacity of remote, unattended
48 observation systems to better capture the atmospheric background in these critical areas (Köne and
49 Büke, 2010).

50 Autonomous and unattended atmospheric observation technology has achieved initial applications
51 across multiple global spheres. Its core technologies (low-power hardware, automated quality
52 control, and remote data transmission) provide a feasible solution for long-term monitoring in
53 remote/extreme regions. In the marine boundary layer, the autonomous ozone measurement system
54 (equipped with PSI and 2B Technologies sensors) developed by the Woods Hole Oceanographic
55 Institution has successfully operated for over one month in an unattended mode on Atlantic buoys
56 and the Chesapeake Bay Lighthouse Tower, thanks to its waterproof packaging, automatic valve
57 protection (to cope with high winds and sea fog), and fault self-correcting controller. Among them,
58 the 2B sensor consumes less than 4 W of power, which is compatible with the energy constraints
59 of marine platforms (Hintsa et al., 2004). In the atmospheric background monitoring at fixed
60 terrestrial stations, the 300-meter tall tower station in Bialystok, Poland, has implemented
61 quasi-continuous observations of multiple species such as CO₂, O₂/N₂, and CH₄ since 2005. By
62 automatically calibrating the CO₂/O₂ sensors every 40 hours, the gas chromatography module
63 every 5 days, and conducting weekly flask sampling for quality control, the station has ensured
64 data continuity for more than 3 years. Additionally, multi-height sampling has enabled effective
65 differentiation between local and regional GHG signals (Popa et al., 2010). In the field of mobile
66 observation, the MPAL vehicle-mounted monitoring platform of the University of Michigan
67 achieves 6.5 hours of continuous operation of all instruments relying on LiFeMnPO₄ battery packs.
68 Through automatic PM sampling loss correction and weekly comparison with fixed stations, it
69 completed 84 days of observations with over 260,000 1-second resolution data points in Detroit,
70 verifying the spatiotemporal coverage advantages of mobile unattended platforms (Xia et al.,
71 2023). Furthermore, the REA-FTIR flux system at the Shoalhaven Farm in Australia completed 3
72 weeks of unattended simultaneous flux observations of CO₂, CH₄, and N₂O relying on 3G remote
73 monitoring and automatic sampling bag switching, and also proposed an innovative method for
74 estimating N₂O background fluxes via CO₂ tracer (Griffith et al., 2009).

75 The observation of greenhouse gases and other atmospheric components in Antarctica presents
76 significant challenges, particularly regarding conducting unattended monitoring. The extreme
77 environmental conditions, including low temperatures, strong winds, and long periods of darkness,
78 pose technical difficulties for maintaining continuous observation systems (Griffiths et al., 2020).
79 Moreover, logistical support in such a remote region is limited, making it hard to deploy and
80 maintain equipment effectively. Over the years, targeted efforts have been made to address these
81 challenges, with some advances in equipment adaptation, energy management, and data reliability:
82 (1) British Antarctic Survey (BAS) Autonomous Ozone Network (2007–present): BAS deployed
83 a network of 2B Technologies ozone monitors (ultraviolet photometry, 5 min sampling interval,
84 11–13 W power consumption) across 8 sites, from the southeastern coast of the Weddell Sea to the
85 Antarctic Plateau (Bauguitte et al., 2011). The system relied on "solar-wind hybrid power +
86 lead-acid batteries" (10–14 days of backup) and passive insulation with intake heating to avoid



87 icing. It delivered 5 years of continuous data (2007–2012), with spring ozone concentrations
88 averaging 28 ± 3 ppb along the coast (vs. 35 ± 2 ppb on the plateau) and a data continuity rate of
89 85%. This work first confirmed that ozone depletion rates were higher at polar vortex edges (0.8
90 ppb/day) than inland (0.3 ppb/day). However, limitations emerged: passive insulation failed at
91 -60°C (causing 15% winter data loss), wind turbine blade icing halted power supply for 12
92 consecutive days in 2009, and the lack of automatic calibration required manual on-site
93 zero-checks, increasing operational costs (Bauguitte et al., 2011).

94 (2) Chinese Kunlun Station (Dome A) Ozone Monitoring (2016): During the 2016 Chinese
95 National Antarctic Research Expedition (CHINARE), Ding et al. (2020a) deployed a 2B
96 Technologies Model 205 ozone monitor (10 min sampling interval, 5 W power consumption) at
97 Dome A (80.25°S), leveraging the PLATO astronomical observatory module's shared diesel
98 generator and 50 kWh battery for power. The instrument operated continuously for 1 year,
99 capturing the first annual ozone dataset for Antarctica's highest-latitude inland region—with polar
100 night concentrations averaging 32 ± 4 ppb and summer concentrations 29 ± 2 ppb (15% lower than
101 at Dome C). Data continuity reached 99.5%, validating the Model 205's suitability for extreme
102 cold. Nevertheless, the system suffered from energy dependency (Ding et al., 2020a).

103 (3) Terra Nova Bay Station Stratospheric NO_2 Monitoring (2000): Bortoli et al. (2002) deployed a
104 GASCOD UV-Visible spectrometer (423–460 nm wavelength, 0.5 nm resolution) at Terra Nova
105 Bay Station for unattended NO_2 observations. Key adaptations included a 30° inclined quartz
106 window to reduce snow accumulation, 24-hour continuous measurement (with integration time
107 auto-adjusted from 2–5 seconds at noon to 5–10 minutes at twilight), and a built-in mercury lamp
108 for daily grating calibration (spectral accuracy < 0.2 nm). Invalid data were screened via the "Flux
109 Index (FI)" (values $< 5 \times 10^{-5}$ mV/ms rejected). The system yielded 1996 data showing NO_2 slant
110 column densities (sc) dropping from 1.2×10^{17} to 4×10^{16} molecule/cm² in austral autumn and
111 rebounding in spring—confirming coupling between photochemical loss and dynamic transport. It
112 also quantified temperature-dependent errors: NO_2 sc increased by 3.5%–4% for every 10K rise in
113 cross-section temperature. However, heavy snow in August 1996 covered the quartz window,
114 causing a 7-day data gap, and mercury lamp intensity declined at -10°C , leading to two failed
115 calibrations.

116 The Antarctic inland plateau faces unique challenges including ultra-low temperatures (below
117 -40°C), polar night (over 3 months without effective illumination), and extremely low logistical
118 accessibility. Existing global unattended monitoring schemes (such as solar-powered supply for
119 marine platforms, mains-powered calibration for terrestrial tall towers, and 3G communication for
120 farmland systems) cannot be directly adapted to this region. Therefore, developing a fully
121 automated greenhouse gases and surface ozone observation system tailored to the Antarctic inland
122 plateau, which fills the gap in unattended monitoring of the atmospheric background in the polar
123 inland, is of crucial significance for understanding the polar feedback of the global climate system.
124 Building on these experiences, a new system to monitor greenhouse gases and surface ozone was
125 developed in 2022/2023 and deployed at the Antarctic inland Taishan Station. But it only lasts 3
126 days for its high requirement on power consumption (The energy consumption of the temperature
127 control module accounts for 70%, 3 kW at the peak.), which leads to overloading of the green
128 power generation device. As a result, an improved system named CRUX-1.0 (The name "CRUX"
129 is inspired by constellation of Crux is one of the most prominent and easily recognizable
130 constellations in the southern hemisphere sky) was developed with 350 W power limitation and



4

131 tested at Tulihe, China, during cold season (- 20 to -40 °C). Then in February 2024, it was
132 deployed at Taishan Station on the Antarctic ice sheet. This system successfully operated for one
133 month before the power supply broke down, providing valuable data on the atmospheric
134 composition in this extreme environment. Here in this paper, we will introduce the detailed design
135 of the system and its performance in Antarctica.

136 **2 Site Descriptions**

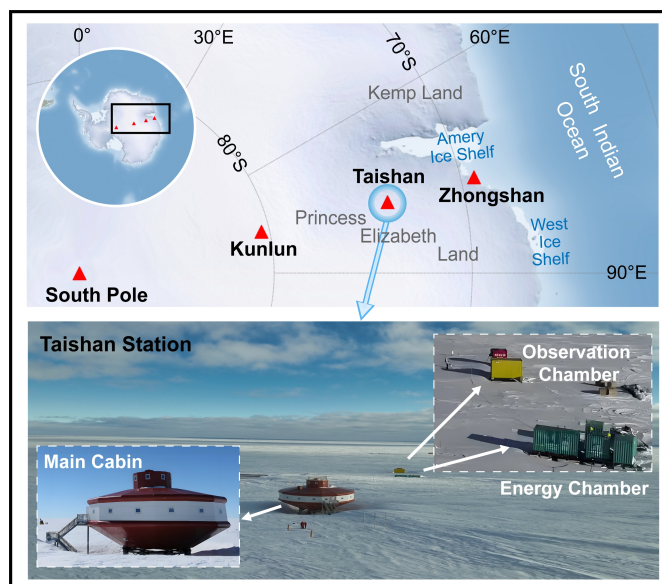
137 Atmospheric CO₂ and O₃ observational data in this study were obtained from one self-developed
138 unattended monitoring system and four WMO-certified long-term monitoring stations with mature
139 observation networks. The authoritative sources and verification channels for 2024 observational
140 data are specified as follows: CO₂ data were retrieved from the World Data Centre for Greenhouse
141 Gases (WDCGG) of the World Meteorological Organization/Global Atmosphere Watch
142 (WMO/GAW, <https://gaw.kishou.go.jp/data/>), while surface ozone data were derived from the
143 European Database for Atmospheric Sounding (EBAS,
144 <https://ebas-data.nilu.no/Pages/DataSetList.aspx>). All datasets were verified via the WMO/GAW
145 quality control system to ensure cross-station consistency and comparability (World
146 Meteorological Organization [WMO], 2018; Montzka et al., 2015; Platt & Lunder, 2024).

147 **2.1 Taishan Station**

148 Taishan Station (72.01°S, 92.08°E; 2621 m a.s.l.) is located on the Antarctic ice sheet (Figure 1). It
149 is situated on the high Antarctic Plateau, an area characterized by extreme environmental
150 conditions. The station experiences strong katabatic winds and is positioned in a region with
151 limited access to logistics and power resources, making it a challenging site for long-term
152 atmospheric monitoring. The climate at Taishan Station is typical of the high Antarctic interior,
153 where temperatures are consistently low throughout the year. The long-term data from September
154 2012 to July 2021 revealed an annual average air temperature of -35.4°C, with a relative humidity
155 of 67%, an air pressure of 699 hPa, and an average wind speed of 10.9 m/s (Ding et al., 2022). The
156 temperature exhibits significant seasonal variation, with a clear "coreless" winter, meaning that
157 there is no distinct temperature minimum, which is common in the interior of Antarctica due to the
158 unique seasonal sunlight patterns (Figure 2a, b, c, d). Furthermore, temperature variability is much
159 greater during the austral winter (2.46°C) than during the austral summer (1.67°C), reflecting the
160 greater frequency of weather events and atmospheric disturbances during the colder months (Ding
161 et al., 2020b; 2022).



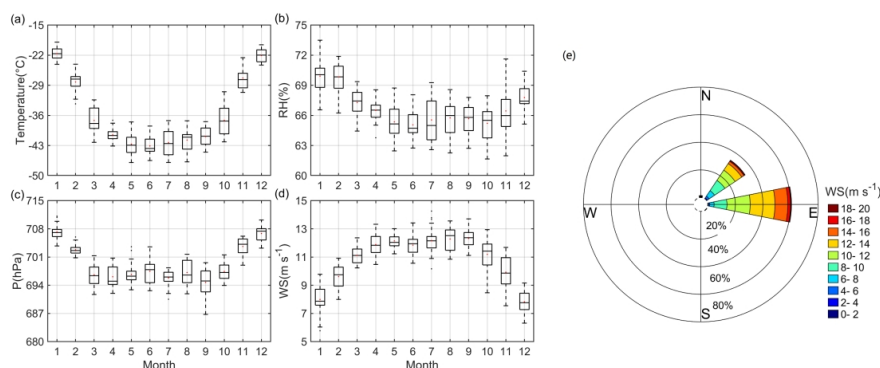
5



162

163

Fig. 1 Geographical distributions of Taishan station



164

165

166

167

168

169

170

171

172

173

174

175

176

177

Fig. 2: Multiyear monthly average temperature (a), relative humidity (b), atmospheric pressure (c), wind speed, and wind direction (d, e) at Taishan Station.

In terms of wind patterns, Taishan Station predominantly experiences easterly winds throughout the year, with gusts reaching more than 20 m/s (Figure 2e). During the summer months, persistent easterly winds dominate the region, whereas in winter, the wind direction shifts from northeast to southeast due to katabatic forces, large-scale pressure gradients, and the Coriolis effect. These conditions contribute to significant challenges such as blowing snow, which can further affect a station's operations and observations (van den Broeke and van Lipzig, 2003; van den Broeke et al., 2002).

The CRUX-1.0 fully automated unattended observation system was deployed at Taishan Station from February 10 to March 9, 2024. This system has achieved simultaneous monitoring of CO₂ and O₃ and obtained continuous observation data. Specifically, the CRUX-1.0 system is installed in a yellow observation cabin, which is located approximately 100 meters to the southeast of the



178 green-colored unattended generator cabin (Figure 1). Given that easterly winds prevail at Taishan
179 Station, the air inlet of the observation cabin is positioned on the upwind side of the generator
180 cabin, which effectively minimizes the potential interference of the monitoring results from the
181 exhaust emissions of the generator cabin. Detailed technical parameters and operational
182 mechanisms of this system will be elaborated in Section 3.

183 2.2 Other Observation Stations

184 2.2.1 South Pole Station

185 Amundsen-Scott South Pole Station (SPO; 90°S, 24.8°W; 2837 m a.s.l.) is a manned baseline
186 station located at the geographic South Pole, representing the coastal-inland transitional
187 atmospheric conditions of Antarctica. Atmospheric CO₂ and O₃ are monitored using in-situ
188 GC-MS and UV spectrometers with a 1-h sampling frequency, operated by the NOAA Global
189 Monitoring Laboratory. Air samples are collected biweekly in paired glass flasks for offline
190 verification, with weekly automatic calibration against NOAA-2016 standard scales (Montzka et
191 al., 2015; Mahesh et al., 2003). The station's data continuity rate is 98.8%, and its observations are
192 widely recognized as a benchmark for Antarctic coastal atmospheric background (Prinn et al.,
193 2018).

194 2.2.2 Barrow Station

195 Barrow Station (BRW; 71.32°N, 156.61°W; 11 m a.s.l.), operated by NOAA's GMCC program, is
196 a key Arctic coastal background station. The station monitors CO₂ and O₃ with NDIR analyzers
197 and UV spectrometers at a 1-h temporal resolution, with additional flask sampling every 2 weeks
198 for cross-validation. Affected by North American regional emissions and Arctic atmospheric
199 circulation, BRW captures both baseline Arctic air masses and episodic pollution transport events
200 (e.g., Eurasian arctic haze; Bodhaine et al., 1981). Data from BRW were averaged to 10-min
201 intervals, with QC procedures following NOAA's standard protocols (Dutton et al., 2002).

202 2.2.3 Mauna Loa Station

203 Mauna Loa Station (MLO; 19.54°N, 155.58°W; 3397 m a.s.l.) is a global benchmark mid-latitude
204 marine background station, operated by NOAA since 1958. Its CO₂ observations provide the
205 longest continuous record of atmospheric greenhouse gas concentrations worldwide, with
206 measurements conducted via hourly NDIR analysis and daily flask sampling. O₃ is monitored
207 using UV absorption sensors with 1-h resolution, calibrated against WMO GAW standards. The
208 station's remote location on the Hawaiian volcanic summit, dominated by westerly winds from the
209 Pacific Ocean, minimizes local anthropogenic interference, making it ideal for capturing
210 mid-latitude baseline atmospheric conditions (Keeling et al., 1976).

211 2.2.4 Jungfraujoch Station

212 Jungfraujoch Station (JFJ; 46.54°N, 7.96°E; 3580 m a.s.l.) is a high-altitude mid-latitude alpine
213 background station in the Swiss Alps, managed by the ACTRIS network. It conducts in-situ
214 monitoring of CO₂ (via Mairak broad-band infrared analyzers) and O₃ (via UV spectrometers)
215 with a 6-min averaging frequency, supplemented by weekly flask sampling. The station is
216 sensitive to European regional atmospheric circulation and photochemical activity, capturing
217 distinct diurnal and seasonal fluctuations in trace gas concentrations (Kubistin et al., 2014). Data
218 consistency is maintained through monthly cross-calibration with reference gas mixtures, with a
219 long-term data completeness rate of ~92% (affected by alpine extreme weather; Sturm et al.,
220 2012).

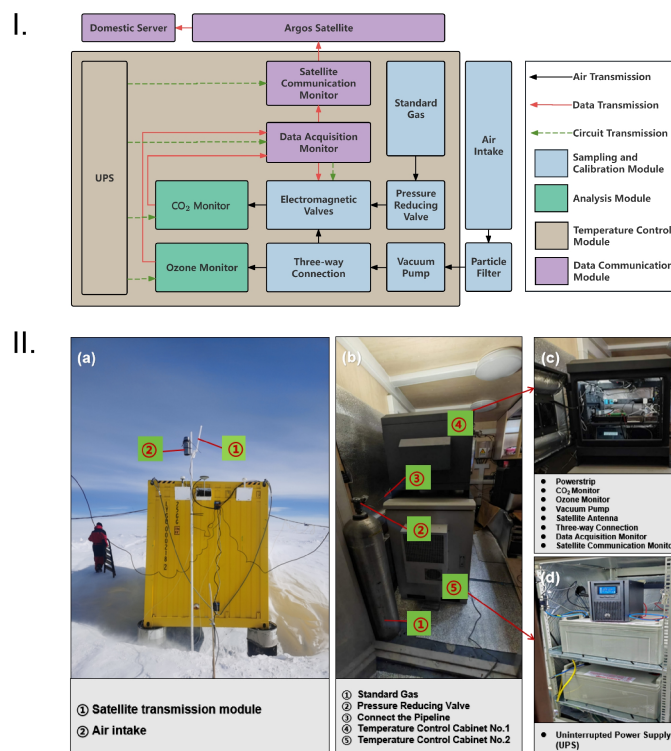
221 Despite minor calibration scale differences across networks (e.g., NOAA vs. ACTRIS), previous



222 studies have confirmed that inter-network biases are <1% for CO₂ and <3% for O₃, which are
 223 negligible for regional and global comparative analyses (Prinn et al., 2018; Wu et al., 2001).

224 **3. Design of the observation system**

225 The preliminary version of the unmanned automatic observation system, CRUX-1.0, is designed
 226 with 4 main modules: a sampling and calibration module, an analysis module, a temperature
 227 control module and a data communication module.



228
 229 Fig. 3 Functional and structural layout (I) and onsite installation and layout (II) of the unmanned
 230 automated CO₂ and surface ozone observation system at Taishan Station

231 **3.1 Sampling and Calibration Module**

232 **3.1.1 Sampling**

233 The sampling module is responsible for collecting atmospheric gas samples and ensuring their
 234 consistent flow into the analysis module for evaluation (see Figure 3-I). It consists of several key
 235 components that work together to maintain a stable and reliable system. The intake port,
 236 positioned at a height of 2.9 m (see Figure 3-II-a), ensures that the air samples are representative
 237 of the surrounding atmosphere and not influenced by local pollutants or snow. The intake port is
 238 also equipped with a particle filter to prevent the intake of snowflakes, dust, and other large
 239 particles that could contaminate the samples. This elevated position and filter are crucial for
 240 ensuring that the collected data are as accurate as possible.

241 The gas flow controller, which includes a vacuum pump (Kamoer KZP-PE model: low rate ≥7
 242 L/min; power ≤12 W; positive pressure ≥0.2 MPa), standard gas cylinder pressure-reducing valve,
 243 and flow controller, ensures that the gas is drawn into the system at a constant rate (see Figure



244 3-II-b,c). The vacuum pump helps maintain a positive pressure airflow, whereas the flow
245 controller regulates the gas flow for consistent sampling. Additionally, the system incorporates
246 three-way and electromagnetic valves to allow the sampling system to switch between different
247 sampling points or introduce calibration gases as needed. The overall design of the sampling
248 module considers the dominant wind direction at Taishan Station, with the intake positioned in the
249 upwind direction of the energy bin to minimize contamination from emissions. This thoughtful
250 design ensures that the sampling module operates efficiently, even in harsh Antarctic
251 environments.

252 3.1.2 Calibration

253 The calibration module is designed to eliminate instrument drift through standard gas calibration,
254 ensuring the accuracy and stability of the observation data. The standard gas cylinder
255 pressure-reducing valve controls the output pressure of the standard air, with the secondary gauge
256 set to 1 psi. This setting ensures that the instrument's intake pressure is met while conserving the
257 standard air as much as possible, thereby extending its usage duration. Each standard gas cylinder
258 is certified for high precision and traceability and is equipped with a single-stage
259 pressure-reducing valve. The cylinders are connected to the electromagnetic valve via 1/8-inch
260 stainless steel tubing, ensuring the stability of the gas concentrations during transmission.

261 The electromagnetic valve is powered and controlled by the CR1000 data logger, which operates
262 the valve at scheduled intervals through a prewritten control program. This program switches
263 between external air and standard air intake, ensuring a consistent and controlled flow. To
264 maintain a constant airflow through the instrument, a flow controller is installed downstream of
265 the electromagnetic valve, preset to a constant flow rate. This ensures precise control over the gas
266 flow entering the monitoring sensors, improving the accuracy of the measurements.

267 To prevent instrument drift from affecting the observation data, the system incorporates a standard
268 gas calibration system, following the atmospheric background observation guidelines. The data
269 logger sends instructions to the electromagnetic valve to allow standard air to flow into the system
270 twice daily—every 11 hours for a 5-minute period. This calibration process ensures that the sensor
271 is calibrated and that any drift is corrected while considering the limitations of energy
272 consumption and the unmanned operating conditions at Taishan Station.

273 3.2 Analysis Module

274 3.2.1 CO₂ Monitor

275 To meet the energy consumption requirements at Taishan Station (where the atmospheric
276 composition monitoring system needs to maintain a power consumption of less than 0.5 kW), a
277 low-power LICOR-830 CO₂ analyzer (see Figure 3-II-c) is used in this experimental system. This
278 device operates via the nondispersive infrared (NDIR) method, which consumes approximately 20
279 W of power. The NDIR method is considered one of the simplest yet effective technologies for gas
280 detection because of its moderate sensitivity and fast response time. The LICOR-830 is widely
281 used in various research fields, including agronomy, ecology, global carbon cycling, and climate
282 change studies (Griffiths, 1983; Ekeberg, 2004; Chen et al., 2010).

283 The core components of the analyzer include an infrared light source, a light chamber, filters, and
284 a detector. The working principle is as follows: infrared radiation emitted by the light source
285 passes through the target gas in the light chamber. If the spectrum of the radiation overlaps with
286 the absorption spectrum of the target gas, the gas absorbs photons at specific wavelengths
287 according to the Beer–Lambert law (Kwon et al., 2009). After passing through the gas, the



288 infrared radiation is filtered so that only the wavelengths absorbed by the gas are retained. These
289 specific photons, which contain concentration information, are detected by the sensor, and the
290 signal is processed to display the concentration of the greenhouse gas (Xu et al., 2022).

291 Prior to deployment at Taishan Station, a preexpedition laboratory experiment was conducted to
292 quantify the precision differences between the LICOR-830 and the Picarro G2301 greenhouse gas
293 analyzers. This experiment aimed to assess the performance of observation systems based on
294 different principles for measuring greenhouse gases (Nan et al., 2024). Through repeatability tests,
295 drift tests, and target gas calibration tests, it was found that the accuracy of the LICOR-830, after
296 calibration, met the WMO requirement of less than 0.1 ppm and was comparable to the advanced
297 international accuracy level of the Picarro G2301, demonstrating its significant application
298 potential in greenhouse gas monitoring.

299 3.2.2 Ozone Monitor

300 For ozone monitoring, a Model 205 ozone monitor from 2B Technologies (see Figure 3-II-c) was
301 used in this experiment. This model was previously deployed in a year-long ground-based ozone
302 observation experiment at Kunlun Station in Antarctica in 2016, where it successfully collected
303 comprehensive observational data (Ding et al., 2022). Model 205 has demonstrated excellent
304 applicability in ozone concentration monitoring, both domestically and internationally. It is energy
305 efficient, highly accurate, compact, and lightweight, making it an ideal tool for monitoring
306 atmospheric ozone concentrations in outdoor or field environments (Ollison et al., 2013; DiGangi
307 et al., 2018; Tian et al., 2022).

308 The Model 205 ozone monitor operates via ultraviolet photometry (Williams et al., 2006). The
309 ozone concentration was measured by detecting its maximum absorption at a UV wavelength of
310 253.7 nm. When an air sample enters the instrument's gas flow system at a constant flow rate, two
311 electromagnetic valves alternate in directing the sample either into the absorption chamber or
312 through an ozone filter before entering the absorption chamber. The absorption chamber
313 concentrates stable UV light produced by the UV light source. Owing to the absorption
314 characteristics of ozone at 254 nm, the intensity of transmitted light as the gas passes through the
315 chamber is detected, providing accurate and stable measurements of the ozone concentration.
316 Instruments based on this method are widely used in pollution monitoring, including atmospheric
317 and water pollution (Tanimoto et al., 2006).

318 Calibration of the ozone monitor requires an ozone calibration instrument that meets international
319 traceability standards. Therefore, cross-concentration calibrations are performed every three
320 months according to observation protocols. However, the calibration procedures for Antarctic ice
321 sheet instruments differ from those at manned stations. For instance, in 2011, after the BAS team
322 retrieved all instruments from the observation network to Halley Station, they validated them
323 using the newly calibrated TE-Model 49C. Upon returning to Cambridge, the instruments were
324 re-calibrated using the NPL-certified TE-Model 49iPS, confirming that the calibration parameters
325 of the 10 instruments remained stable throughout the year's deployment, with data deviations not
326 exceeding the initial accuracy range of 2% (Bauguitte et al., 2011). In 2016, testing at Antarctic
327 Dome A confirmed the stable operation of the instrument in the field, and reliable observations can
328 be obtained by conducting calibrations twice per year (Ding et al., 2020a). Owing to the overall
329 energy consumption limitations and unattended conditions at Taishan Station, we conducted two
330 calibrations, one before and one after the observation experiment, with data deviations not
331 exceeding the initial accuracy range of 2%.



332 3.3 Temperature Control Module

333 The temperature control module is designed to ensure the stable operation of the monitoring
334 equipment under extreme Antarctic conditions, especially the freezing temperatures at Taishan
335 Station. This module includes a temperature control cabinet, a gas flow controller, and an
336 uninterruptible power supply (UPS) (see Figure 3-II-b-4, 5). The temperature control cabinet is
337 equipped with precise sensors and adjustment mechanisms that maintain a stable internal
338 temperature range for the equipment, protecting it from extreme cold at the station.

339 To meet the appropriate temperature range for the operation of CO₂ and ozone monitoring while
340 reducing the energy consumption of temperature control, the minimum heating temperature of the
341 temperature control cabinet is preset to 10°C. When the internal temperature drops below 10°C,
342 the system begins to heat; when the temperature exceeds 15°C, heating stops, ensuring that the
343 equipment remains within a safe and optimal operating temperature range. This design ensures
344 that the monitoring instruments are effectively protected in the extremely low-temperature
345 environment of Taishan Station (which can reach as low as -40°C). The environmental monitoring
346 and control system, which includes temperature regulation, is the highest power-consuming
347 component in the entire system, with a peak power consumption of 250 W. Given the power
348 constraints at Taishan Station, energy efficiency is a crucial consideration in the design of the
349 temperature control system. This is balanced with the need to maintain a stable environment for
350 the equipment.

351 Since the experimental system is powered by Taishan Station's external energy cabin, an
352 uninterruptible power supply (UPS) system is installed to prevent sudden power outages or
353 voltage instability from negatively impacting the system's operation (Figure 3-II-d). The UPS
354 provides stable and reliable power to the entire monitoring system (see Figure 3-II-d). In the event
355 of an external power failure, the UPS can quickly switch to backup power. The battery backup can
356 last up to 48 hours, ensuring the continuous operation of the monitoring system and uninterrupted
357 data collection. This design significantly enhances the system's reliability and fault tolerance,
358 providing a safeguard against power disruptions in the remote environment.

359 3.4 Data Communication Module

360 The satellite communication system consists of a customized bracket (with a height of 3 m) and an
361 integrated transmitting antenna (Figure 3-II-a-1), enabling high-speed and stable data
362 transmission to a remote data center. This module uses ARGOS satellite communication
363 technology, ensuring the real-time transmission of monitored data processed by the data logger in
364 the harsh Antarctic environment, which can avoid potential interruptions and delays that could
365 arise with traditional ground communication methods. The stable applicability of this satellite
366 communication module in Antarctica has been verified through testing at the Prydz Bay-Amery
367 Ice Shelf-Dome A (PANDA) profile automatic weather station (Ding et al., 2022).

368 The data processing and storage system uses the CR1000X measurement and control data logger
369 (see Figure 3-II-c), a low-power device primarily used for sensor measurements, direct/remote
370 communication connections, data analysis, external device control, and storage of data and
371 programs. It features a sealed design to shield against radio frequency interference and a stainless
372 steel housing. Equipped with a precise clock, it supports the BASIC-like programming language
373 commonly used by Campbell Scientific data loggers, which includes data processing and analysis
374 capabilities.

375 The CR1000X connection panel has two 12 V terminals, 16 analog measurement terminals, and

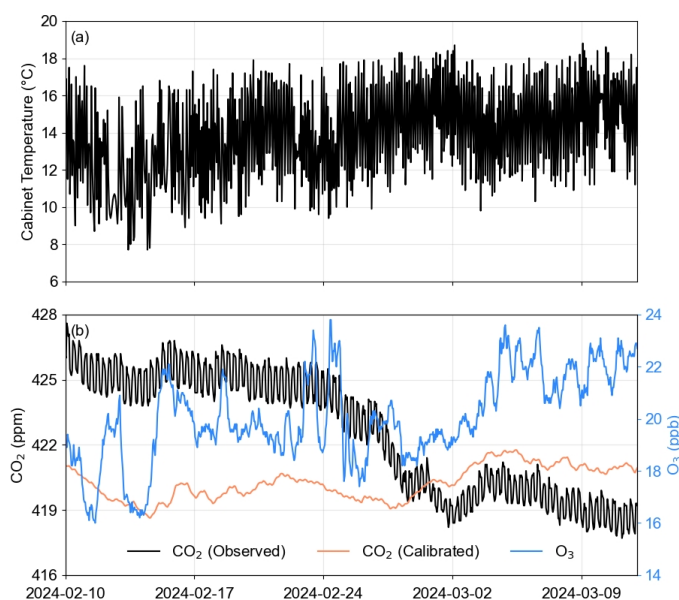


376 detachable connectors. It is responsible for receiving raw data from two monitoring sensors,
377 performing preprocessing, analysis, and storage. This module has powerful data processing
378 capabilities, enabling it to filter out and correct anomalous data points in real time, ensuring the
379 reliability of the data quality. Additionally, the module supports remote data access and download
380 functions, allowing researchers to retrieve and analyze monitoring data at any time.

381 4. Experimental analysis

382 4.1 Observational results

383 From February 10 to March 12, 2024, the observation system at Taishan Station operated
384 autonomously under unattended low-temperature conditions, with good performance, and satellite
385 remote data transmission was normal. By analyzing the transmitted data, we found the following:
386 in the environment at Taishan Station, where the average temperature was below -25°C in
387 February, the internal temperature of the equipment cabinet was able to be stably maintained at
388 $13.9 \pm 2.5^{\circ}\text{C}$ (Figure 4a), meeting the environmental temperature requirements for both types of
389 optical cavity equipment used in this experiment.



390

391 Fig. 4 Cabinet temperature (a), hourly average concentration of observed CO₂, hourly average
392 concentration of calibrated CO₂ and O₃ concentration transmitted from the unattended automated
393 observation system at Taishan Station (b).

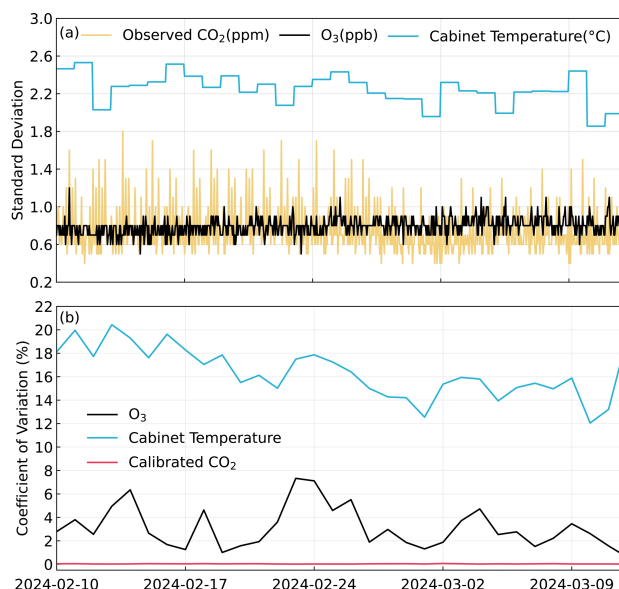
394 From February 10 to March 12, 2024, the hourly average concentration of observed CO₂ at
395 Taishan Station was 422.6 ± 2.8 ppm (Figure 4b). To ensure the accuracy of the observation data,
396 the system automatically introduces standard gas every 11 hours for 10 minutes to correct the
397 instrument measurement deviation. After data quality control, the daily average concentration of
398 calibrated CO₂ at Taishan Station was 420.3 ± 1.5 ppm.

399 4.2 Accuracy evaluation

400 To assess the overall performance and stability of the system, we employed the standard deviation
401 and coefficient of variation (CV) as key metrics. The standard deviation provides insight into the



402 dispersion of measurement data, reflecting the precision and stability of the system. On the other
 403 hand, CV, which normalizes the standard deviation by the mean value, allows for a comparison of
 404 variability across different parameters and conditions, regardless of their magnitude. Using these
 405 two metrics, we evaluated the precision of O₃ and CO₂ concentrations, as well as the cabinet
 406 temperature, over time.



407
 408 Fig. 5 Evaluation of the Precision of O₃ and CO₂ Concentrations and Cabinet Temperatures
 409 through Standard Deviation and Coefficient of Variation Analysis Standard Deviation (a)
 410 Coefficient of Variation (b)

411 The O₃ concentration (black line) consistently has a low standard deviation and minimal
 412 fluctuations, indicating high measurement stability. In contrast, the original CO₂ concentration
 413 (yellow line) displays substantial variation, with a peak standard deviation of 1.8, suggesting
 414 lower precision (Figure 5a). The cabinet temperature (blue line) maintains a stable standard
 415 deviation, although a stepwise decrease over time suggests some control, albeit with potential for
 416 further improvement. In terms of the CV, the O₃ concentration remains low (<6%) and continues
 417 to decrease over time, reflecting enhanced measurement consistency. Postcalibration, the CO₂
 418 concentration (red line) significantly decreases in CV, approaching 0%, demonstrating the
 419 effectiveness of calibration in improving measurement accuracy. However, the cabinet
 420 temperature shows a higher CV (~16%-20%), indicating notable fluctuations, possibly due to
 421 environmental factors or temperature control system design (Figure 5b). Overall, while O₃
 422 concentration measurements demonstrate high precision and stability, CO₂ concentration precision
 423 improves substantially with calibration. Temperature control remains stable but requires
 424 optimization to reduce variability and further improve measurement accuracy.

425 **5. Discussion**

426 **5.1 Performance Comparison**

427 Traditional manned stations (e.g., South Pole Station) have irreplaceable advantages: real-time
 428 troubleshooting, flexible parameter adjustment, and weekly on-site calibration (measurement



429 uncertainty <0.5 ppm, better than CRUX's ± 1.0 ppm for CO₂). However, manned observations
 430 face high logistics costs and data gaps due to extreme weather evacuations. CRUX compensates
 431 for these shortcomings: its 30-day autonomous operation cuts logistics costs by over 90%, and
 432 48-hour UPS backup ensures data continuity during power outages. The consistency of its results
 433 with South Pole Station (CO₂: 420.3 \pm 1.5 ppm vs. 418.2 ppm; O₃: 20.1 \pm 0.8 ppb vs. 20.5 ppb)
 434 confirms it can provide comparable data quality in stable environments, serving as an effective
 435 supplement to manned observations.

436 **Table 2. Comparison of the Polar Automatic GHG or Ozone Observation Systems**

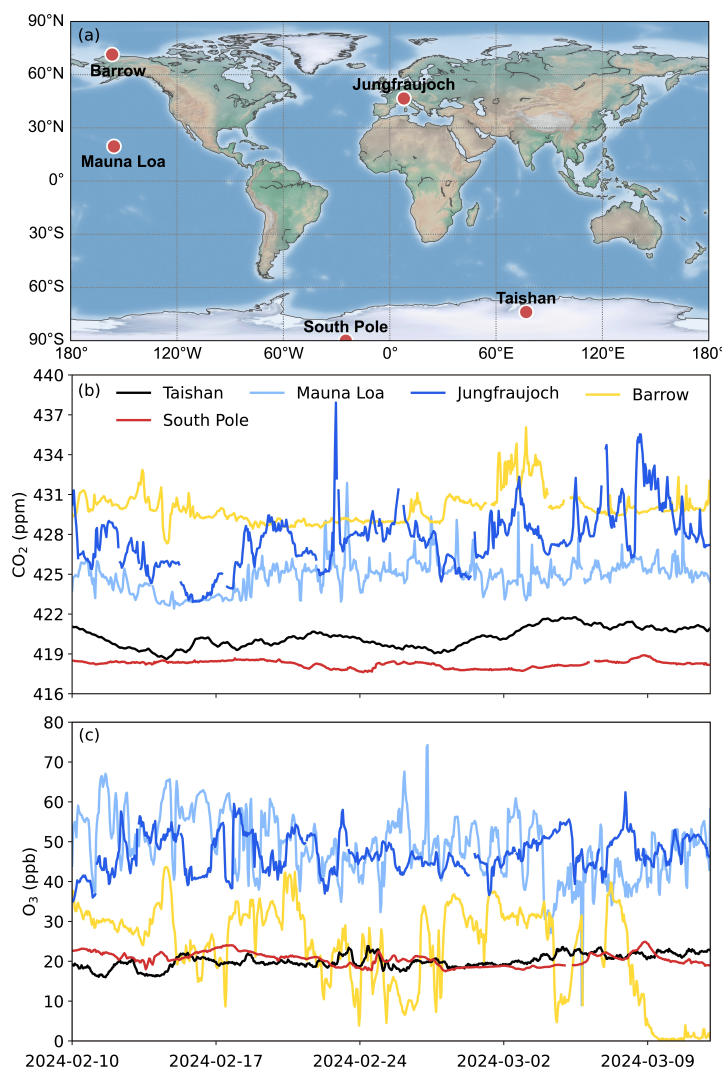
Key Techniques	CRUX-1.0 (2024)	BAS Ozone Network (2011)	Kunlun Station Ozone Monitor (2016)
Monitoring Parameters	CO ₂ / O ₃	O ₃	O ₃
Power Consumption	<350 W	11–13 W	5 W
Temperature Control Method	Auto-temperature control (10–15°C)	Passive Insulation with intake heater	Passive Insulation
Calibration Method	CO ₂ : Automatic (Single standard gas mode, twice daily); O ₃ : Periodic calibration	On-site zero-check with manual intervention and Periodic calibration	Periodic calibration
Single Battery Backup Duration	48 hours (UPS Backup Battery)	10–14 days (Lead-Acid Batteries)	Not applicable
Data Continuity Rate	99.2%	85% (Affected by power/communication)	99.5%

437 As shown in Table 2, CRUX's strengths lie in integrated optimization for Antarctic inland
 438 conditions: (1) Balanced performance: It reduces power consumption by 92% compared to the
 439 initial 3 kW version, achieving <350 W operation while maintaining multi-parameter detection,
 440 adapting to polar green energy constraints. (2) Extreme cold reliability: Active temperature control
 441 isolates -25°C to -40°C external temperatures, and upwind intake with particle filters mitigates
 442 blowing snow interference. (3) High autonomy and accuracy: Twice-daily auto-calibration reduces
 443 CO₂ CV to near 0%. Field tests revealed non-negligible flaws: (1) Temperature control lag: A
 444 5-minute heating response delay leads to 16%–20% cabinet temperature CV, potentially causing
 445 0.2 ppm/h drift of the LICOR-830 analyzer. (2) Insufficient long-term power: 48-hour UPS
 446 backup. (3) Limited adaptability: Fixed-time calibration cannot respond to sudden sensor drift;
 447 only two parameters are monitored.

448 **5.2 Site Comparison**



449 To interpret the observational results from Antarctic Taishan Station in a global context and assess
450 the performance of the CRUX-1.0 unattended system, a comparative analysis was conducted on
451 concurrent CO₂ and O₃ datasets from five global atmospheric background stations, which differ in
452 geographical locations (polar vs. mid-latitude) and operational modes (unattended vs. manned).
453 The selected stations include Taishan Station (Antarctic inland, unattended), South Pole Station
454 (Antarctic coastal, manned), Barrow Station (Arctic coastal, manned), Mauna Loa Station
455 (mid-latitude marine, manned), and Jungfraujoch Station (mid-latitude alpine, manned) (Figure
456 6a).



457

458 Fig. 6 Global distribution of selected atmospheric background stations (a) and their concurrent

459 CO₂ (b) and O₃ (c) observations (2024-02-10 to 2024-03-12)

460 Comparative results revealed distinct regional and operational differences in both CO₂ and O₃

461 observations. For CO₂, polar stations (Taishan and South Pole; mean: 420.2 and 418.2 ppm;



462 hereafter means) exhibited significantly lower baseline concentrations than mid-latitude
463 counterparts (Mauna Loa: 424.9 ppm; Jungfraujoch: 427.6 ppm), primarily due to the absence of
464 anthropogenic emissions in the Antarctic inland. Taishan Station also showed smaller fluctuation
465 amplitude (± 1.5 ppm), attributed to the homogeneous air masses in the Antarctic inland circulation
466 and interference-free operation of the unattended system, whereas mid-latitude stations displayed
467 larger fluctuations driven by regional emission transport and diurnal cycles. For O_3 , polar stations
468 (Taishan: 20.1 ppb; South Pole: 20.5 ppb) had much lower concentrations than mid-latitude
469 stations (Mauna Loa: 48.9 ppb; Jungfraujoch: 47.1 ppb), which was associated with weak
470 photochemical activity in the Antarctic late summer, which was associated with the low
471 concentrations of ozone precursors in Antarctica (due to the dual scarcity of natural and
472 anthropogenic sources) impair the ozone formation potential, while the intense sunlight in summer,
473 chemical depletion triggered by trace amounts of NO , and stable boundary layer conditions jointly
474 lead to surface ozone in Antarctica being dominated by depletion during summer (Tian et al.,
475 2022).

476 Notably, the data continuity rate of Taishan Station (99.2%) was comparable to that of the manned
477 South Pole Station (98.8%), verifying the reliability of the CRUX-1.0 system in extreme polar
478 environments. While mid-latitude manned stations excel in real-time calibration and
479 multi-parameter expansion, the unattended CRUX-1.0 system fills the observation gap in the
480 remote Antarctic inland, complementing the global atmospheric background network. Future
481 optimization could integrate multi-point span calibration techniques from manned stations to
482 enhance automated quality control.

483 6. Summary

484 To explore a new unattended observation model suitable for monitoring greenhouse gases (GHG)
485 and surface ozone (O_3) in the extreme environment of the Antarctic inland plateau, this study
486 developed the CRUX-1.0 fully automated unattended observation system. Integrating four core
487 modules—sampling and calibration, analysis, temperature control, and data communication—the
488 system is specifically optimized for polar conditions, featuring key characteristics such as low
489 power consumption (< 350 W), active temperature control (10 – $15^\circ C$), twice-daily automatic
490 calibration for CO_2 , and 48-hour uninterruptible power supply (UPS) backup. It is adaptable to
491 observation needs in remote areas with low logistical support.

492 Deployed and operated at Taishan Station ($72.01^\circ S$, $92.08^\circ E$) from February 10 to March 9, 2024,
493 the system ran stably for one month with a data continuity rate of 99.2%. The calibrated CO_2
494 concentration was 420.3 ± 1.5 ppm, and the O_3 concentration was 20.1 ± 0.8 ppb, which were highly
495 consistent with the concurrent manned observation results at South Pole Station. After calibration,
496 the coefficient of variation (CV) for CO_2 was near 0%, and for O_3 was $< 5.6\%$, successfully
497 verifying the reliability and feasibility of the unattended model for observations in extreme polar
498 environments.

499 Compared with traditional manned stations, CRUX-1.0 achieves observation data of comparable
500 accuracy at less than 90% of the logistical costs, providing a flexible and complementary new
501 technical solution for the global polar observation network and facilitating the development of
502 polar atmospheric background monitoring towards low-cost and wide-coverage. Currently, polar
503 unattended observations still face common technical challenges, including temperature control
504 precision, long-term energy supply, multi-parameter simultaneous monitoring, and dynamic
505 calibration. In the future, joint efforts from academia and industry are urgently needed: promoting



16

506 the precision development of temperature control technologies for ultra-cold environments,
507 exploring solar-wind-energy storage integrated hybrid energy systems for polar regions,
508 developing multi-component collaborative observation modules and intelligent dynamic
509 calibration algorithms, and further enhancing the extreme adaptability and observational
510 comprehensiveness of unattended systems. This will provide more abundant polar atmospheric
511 background data support for global climate change research.

512

513 **Data availability**

514 The in-situ observational datasets generated in this study, including the hourly raw and calibrated
515 CO₂ and O₃ concentration data from the CRUX-1.0 system at Taishan Station, Antarctica, the
516 system operation and temperature control records, and the data quality control results, are
517 available from the corresponding author upon reasonable request. The reference CO₂ datasets for
518 global background stations were retrieved from the World Data Centre for Greenhouse Gases
519 (WDCGG) of WMO/GAW (<https://gaw.kishou.go.jp/data/>), and the surface ozone datasets were
520 obtained from the European Database for Atmospheric Sounding (EBAS,
521 <https://ebas-data.nilu.no/Pages/DataSetList.aspx>). Both public datasets are accessible in
522 compliance with their respective official data policies.

523

524 **Author contributions**

525 Biao Tian was responsible for funding acquisition, field experiment, writing of the original draft,
526 experimental design, and formal analysis. Minghu Ding was responsible for project administration,
527 supervision, resources coordination, and review and editing. Kongju Zhu and Xu Yao were
528 responsible for on-site field experiment. Yixi Zhao was responsible for formal analysis and data
529 visualization. Wenqian Zhang was responsible for system software debugging and remote data
530 acquisition. Diyi Yang, Weijun Sun, Yining Yu, Shoudong Zhao, Yige Cui, Chuanjin Li, Jie Tang,
531 Cunde Xiao, Tong Zhu, and Renhe Zhang were responsible for review and editing.

532

533 **Disclaimer**

534 Publisher's note: Copernicus Publications remains neutral with regard to jurisdictional claims made
535 in the text, published maps, institutional affiliations, or any other geographical representation in
536 this paper. The authors bear the ultimate responsibility for providing appropriate place names.
537 Views expressed in the text are those of the authors and do not necessarily reflect the views of the
538 publisher.

539

540 **Declaration of competing interest**

541 The authors declare that they have no known competing financial interests or personal
542 relationships that could have appeared to influence the work reported in this paper.

543

544 **Acknowledgments**

545 This study was made possible with the support and assistance of the 39th and 40th Chinese
546 National Antarctic Research Expeditions (CHINARE) team. We would like to express our
547 heartfelt gratitude for their invaluable contributions during the data collection process.

548

549 **Financial support**



550 This work is financially supported by the National Natural Science Foundation of China
551 (42201151) and the Basic Research Fund of Chinese Academy of Meteorological Sciences
552 (2023Z004, 2024Z007).

553

554 **References**

555 Bauguitte, S. J. B., Brough, N., Frey, M. M., Jones, A. E., Maxfield, D. J., Roscoe, H. K., Rose, M.
556 C., and Wolff, E. W.: A network of autonomous surface ozone monitors in Antarctica:
557 technical description and first results, *Atmos. Meas. Tech.*, 4, 645–658,
558 <https://doi.org/10.5194/amt-4-645-2011>, 2011.

559 Bodhaine, B. A., Harris, J. M., and Hofmann, D. J.: Arctic haze: a review, *J. Atmos. Sci.*, 38,
560 2311–2327, 1981.

561 Bortoli, D., and Kostadinov, I. K.: Stratospheric ozone and nitrogen dioxide amount obtained with
562 GASCOD-type DOAS spectrometer at Terra Nova Bay Station (Antarctica) during December
563 2000 – January 2001, *Proceedings of SPIE*, 4544, 225–235,
564 <https://doi.org/10.1117/12.454255>, 2002.

565 Chen, H., Winderlich, J., Gerbig, C., Meinhardt, F., Rella, C. W., Crosson, E. R., and Batenburg, A.
566 M.: High-accuracy continuous airborne measurements of greenhouse gases (CO₂ and CH₄)
567 using the cavity ring-down spectroscopy (CRDS) technique, *Atmos. Meas. Tech.*, 3, 375–386,
568 <https://doi.org/10.5194/amt-3-375-2010>, 2010.

569 Das, S. S., Ratnam, M. V., Uma, K. N., Subrahmanyam, K. V., Girach, I. A., Patra, A. K., Aneesh,
570 S., Suneeth, K. V., Kumar, K. K., Kesarkar, A. P., Sijikumar, S., and Ramkumar, G.: Influence
571 of tropical cyclones on tropospheric ozone: possible implications, *Atmos. Chem. Phys.*, 16,
572 4837–4847, <https://doi.org/10.5194/acp-16-4837-2016>, 2016.

573 DiGangi, J., Choi, Y., Nowak, J., and Davis, K. J.: ACT-America: L2 In Situ Atmospheric CO₂,
574 CO, CH₄, and O₃ Concentrations, Eastern USA, ORNL DAAC, Oak Ridge, Tennessee, USA,
575 <https://doi.org/10.3334/ORNLDAAC/1679>, 2018.

576 Ding, M., Tian, B., Ashley, M. C. B., Putero, D., Zhu, Z., Wang, L., Yang, S., Li, C., and Xiao, C.:
577 Year-round record of near-surface ozone and O₃ enhancement events (OEEs) at Dome A, East
578 Antarctica, *Earth Syst. Sci. Data*, 12, 3529–3544, <https://doi.org/10.5194/essd-12-3529-2020>,
579 2020a.

580 Ding, M., Yang, D., van den Broeke, M. R., Allison, I., Xiao, C., Qin, D., and Huai, B.: The
581 surface energy balance at Panda 1 Station, Princess Elizabeth Land: a typical katabatic wind
582 region in East Antarctica, *J. Geophys. Res.-Atmos.*, 125, e2019JD030378,
583 <https://doi.org/10.1029/2019JD030378>, 2020b.

584 Ding, M., Zou, X., Sun, Q., Yang, D., Zhang, W., Bian, L., Lu, C., Allison, I., Heil, P., and Xiao,
585 C.: The PANDA automatic weather station network between the coast and Dome A, East
586 Antarctica, *Earth Syst. Sci. Data*, 14, 5019–5035, <https://doi.org/10.5194/essd-14-5019-2022>,
587 2022.

588 Dutton, E. G., Bodhaine, B. A., and Slusser, J. R.: NOAA's baseline radiation monitoring network,
589 *Bull. Am. Meteorol. Soc.*, 83, 1719–1737, 2002.

590 Ekeberg, D., Ogner, G., and Fongen, H.: Determination of CH₄, CO₂, and N₂O in air samples and
591 soil atmosphere by gas chromatography mass spectrometry, GC-MS, *J. Environ. Monit.*, 6,
592 621–623, 2004.

593 Griffith, D., Petersen, A. K., Naylor, T., Harvey, M., and Smith, M.: Innovative techniques to



- 594 measure greenhouse gas emissions from land systems, Report to the Australian Government
595 Department of Climate Change, 0807, 1–35, 2009.
- 596 Griffiths, P. R.: Fourier transform infrared spectrometry, *Science*, 222, 297–302,
597 <https://doi.org/10.1126/science.222.4621.297>, 1983.
- 598 Griffiths, P. T., Keeble, J., Shin, Y. M., Abraham, N. L., Archibald, A. T., and Pyle, J. A.: On the
599 changing role of the stratosphere on the tropospheric ozone budget: 1979–2010, *Geophys.*
600 *Res. Lett.*, 47, e2019GL086901, <https://doi.org/10.1029/2019gl086901>, 2020.
- 601 Hintsä, E. J., Allsup, G. P., Eck, C. F., Hosom, D. S., Purcell, M. J., Roberts, A. A., Scott, D. R.,
602 Sholkovitz, E. R., Rawlins, W. T., Mulhall, P. A., Lightner, K., McMillan, W. W., Song, J.,
603 and Newchurch, M. J.: New ozone measurement systems for autonomous operation on ocean
604 buoys and towers, *J. Atmos. Ocean. Tech.*, 21, 1007–1016, 2004.
- 605 Keeling, C. D.: Atmospheric CO₂ variations at Mauna Loa Observatory, Hawaii, *Tellus*, 28,
606 538–551, 1976.
- 607 Köne, A. Ç., and Büke, T.: Forecasting of CO₂ emissions from fuel combustion using trend
608 analysis, *Renew. Sustain. Energy Rev.*, 14, 2906–2915,
609 <https://doi.org/10.1016/j.rser.2010.06.006>, 2010.
- 610 Kwon, J., Ahn, G., Kim, G., Kim, J. C., and Kim, H.: A study on NDIR-based CO₂ sensor to apply
611 remote air quality monitoring system, 2009 ICCAS-SICE, 1683–1687, 2009.
- 612 Liu, M., Song, Y., Matsui, H., Shang, F., Kang, L., Cai, X., Zhang, H., and Zhu, T.: Enhanced
613 atmospheric oxidation toward carbon neutrality reduces methane's climate forcing, *Nat.*
614 *Commun.*, 15, 1362, <https://doi.org/10.1038/s41467-024-47436-9>, 2024.
- 615 Mahesh, A., Montzka, S. A., and Dutton, G. S.: Calibration of flask sampling systems for
616 atmospheric trace gas measurements, *J. Atmos. Ocean. Tech.*, 20, 1862–1872, 2003.
- 617 Montzka, S. A., Dutton, G. S., and Hall, B. D.: NOAA's global greenhouse gas reference network,
618 *Bull. Am. Meteorol. Soc.*, 96, 2009–2024, 2015.
- 619 Nan, R. Q., Tian, B., Sun, W. J., Li, C. J., and Ding, M. H.: Comparative study on the precision of
620 greenhouse gas analyzers based on LICOR-830 and Picarro G2301, *J. Shandong Norm. Univ.*
621 *Nat. Sci.*, 39, 52–61, 2024.
- 622 Ollison, W. M., Crow, W., and Spicer, C. W.: Field testing of new-technology ambient air ozone
623 monitors, *J. Air Waste Manag. Assoc.*, 63, 855–863,
624 <https://doi.org/10.1080/10962247.2013.793374>, 2013.
- 625 Platt, U., and Lunder, C. R.: EBAS database quality assurance and control guidelines for ozone
626 measurements, Norwegian Institute for Air Research (NILU), 2024.
- 627 Popa, M. E., Gloor, M., Manning, A. C., Jordan, A., Schultz, U., Haensel, F., Seifert, T., and
628 Heimann, M.: Measurements of greenhouse gases and related tracers at Bialystok tall tower
629 station in Poland, *Atmos. Meas. Tech.*, 3, 407–427, 2010.
- 630 Prinn, R. G., Weiss, R. F., and Miller, B. R.: Intercomparison of AGAGE, NOAA, and SIO
631 atmospheric trace gas calibration scales, *Atmos. Meas. Tech.*, 11, 1587–1601,
632 <https://doi.org/10.5194/amt-11-1587-2018>, 2018.
- 633 Sturm, P., Wanner, H., and Schwikowski, M.: Impact of extreme weather events on high-alpine
634 atmospheric observations at Jungfrauoch, *Atmos. Res.*, 116, 1–12, 2012.
- 635 Tanimoto, H., Mukai, H., Hashimoto, S., and Kajii, Y.: Intercomparison of ultraviolet photometry
636 and gas-phase titration techniques for ozone reference standards at ambient levels, *J.*
637 *Geophys. Res.-Atmos.*, 111, D16305, <https://doi.org/10.1029/2005JD006646>, 2006.



- 638 Tian, B., Ding, M., Putero, D., Li, C., Zhang, D., Tang, J., Zheng, X., Bian, L., and Xiao, C.:
639 Multi-year variation of near-surface ozone at Zhongshan Station, Antarctica, *Environ. Res.*
640 *Lett.*, 17, 044021, <https://doi.org/10.1088/1748-9326/ac583c>, 2022.
- 641 van den Broeke, M. R., van Lipzig, N. P. M., and van Meijgaard, E.: Momentum budget of the
642 East Antarctic atmospheric boundary layer: results of a regional climate model, *J. Atmos. Sci.*,
643 59, 3117–3129, [https://doi.org/10.1175/1520-0469\(2002\)059<3117:MBOTEA>2.0.CO;2](https://doi.org/10.1175/1520-0469(2002)059<3117:MBOTEA>2.0.CO;2),
644 2002.
- 645 van den Broeke, M. R., and van Lipzig, N. P. M.: Factors controlling the near-surface wind field in
646 Antarctica, *Mon. Weather Rev.*, 131, 733–743,
647 [https://doi.org/10.1175/1520-0493\(2003\)131<0733:FCTNSW>2.0.CO;2](https://doi.org/10.1175/1520-0493(2003)131<0733:FCTNSW>2.0.CO;2), 2003.
- 648 Williams, E. J., Fehsenfeld, F. C., Jobson, B. T., and Holloway, J. S.: Comparison of ultraviolet
649 absorbance, chemiluminescence, and DOAS instruments for ambient ozone monitoring,
650 *Environ. Sci. Technol.*, 40, 5755–5762, <https://doi.org/10.1021/es0606353>, 2006.
- 651 World Meteorological Organization (WMO): Global Atmosphere Watch (GAW) measurement
652 guidelines for greenhouse gases, WMO-TD-No. 1881, 2018.
- 653 Wu, C., Prinn, R. G., and Weiss, R. F.: Compatibility of air samples collected in glass and stainless
654 steel flasks for halocarbon measurements, *J. Atmos. Ocean. Tech.*, 18, 1743–1751, 2001.
- 655 Xia, T., Catalan, J., Hu, C., and Batterman, S.: Development of a mobile platform for monitoring
656 gaseous, particulate, and greenhouse gas (GHG) pollutants, *Environ. Monit. Assess.*, 193, 7,
657 <https://doi.org/10.1007/s10661-020-08790-9>, 2023.
- 658 Xu, M., Peng, B., Zhu, X., and Guo, Y.: Multi-gas detection system based on non-dispersive
659 infrared (NDIR) spectral technology, *Sensors*, 22, 836, <https://doi.org/10.3390/s22030836>,
660 2022.
- 661 Yang, D., Ding, M., Dou, T., Han, W., Liu, W., Zhang, J., Du, Z., and Xiao, C.: On the differences
662 in precipitation type between the Arctic, Antarctica, and Tibetan Plateau, *Front. Earth Sci.*, 9,
663 607487, <https://doi.org/10.3389/feart.2021.607487>, 2021.